Malaysian Journal of Science **21A**: 31-40 (2002)

Backdiffraction configuration for x-ray standing wave formed just above the surface of the crystal containing a stacking fault

Hakob P. Bezirganyan[1], Siranush E. Bezirganyan[1], Hayk H. Bezirganyan (Jr.)[2] and Petros H. Bezirganyan (Jr.)[3]

[1] *Faculty of Physics, Yerevan State University, #1, Alex Manoogian Street, Yerevan 375025, Armenia.*
[2] *Faculty of Informatics and Applied Mathematics, Yerevan State University, #1, Alex Manoogian Street, Yerevan 375025, Armenia.*
[3] *Dep. of Computer Science, State Engineering University of Armenia, #105, Terian Street, Yerevan 375009, Armenia.*

ABSTRACT Presented theoretical paper concerns the application of the extremely sensitive Grazing-Angle Incidence X-ray Backdiffraction (GIXB) technique for investigations of the crystal containing a stacking fault. Fault plane is assumed parallel to the crystal entrance surface. It is shown that entire x-ray wave field intensity in vacuum is modulated periodically along the vacuum-crystal surface with the same period as the crystal diffracting net planes. X-ray wave field short-period modulation along the vacuum-crystal surface gives a possibility to determine the lateral positions of overlaid adsorbed atoms with respect to crystal lattice atoms by combination of GIXB with the X-ray Standing-Wave (XSW) technique i.e. by monitoring the secondary emissions. The development of such non-destructive investigation methods is in the focus of fundamental aspects of materials research, crystal engineering etc.

(GIXB, X-ray Standing-Wave, Crystal)

INTRODUCTION

Let consider a model of the crystal extended over the volume $-\infty < x < \infty$; $-\infty < y < \infty$; $z \leq z_1$. Crystal contains a stacking fault. Fault plane $z = z_2$ is parallel to the crystal entrance surface $z = z_1$ (see figure 1). Accordingly, a phase shift x_0 exists between the space periods of perfect crystalline layer and perfect bulk crystal, which are separated by the fault plane (see figure 1). If the thickness $T = z_1 - z_2$ of the perfect crystalline layer is about several nanometers, then the traditional non-destructive methods of investigations becomes non-effective. In general the x-ray investigations can be improved by using the Grazing-Angle Incidence X-ray Backdiffraction (GIXB) technique (e.g. see [1, 2]), which is extremely sensitive to lattice spacing period and radiation wavelength. The GIXB scheme is possible to realise only if the Bragg angle θ_B is close to 90° i.e. GIXB is the Bragg diffraction in the conditions of total external reflection and is superior to conventional x-ray diffraction techniques in the study of the crystal structure of very thin surface layers (see figure 1). The entire wave field intensity in vacuum is modulated along the crystal surface with the same period d as the period of the crystal lattice. This gives an opportunity of determination of the lateral positions of adsorbed atoms along ***Ox***-axis with respect to crystal lattice atoms by combination of GIXB with the X-ray Standing Wave (XSW) technique. XSW method analysed the inelastic scattering response of atoms (e.g. photoelectrons yield, fluorescence radiation, Compton scattering etc.) within the range of an x-ray interference field, i.e. the XSW technique probes the in-plane position of overlaid atoms through observation of secondary emission profiles using the x-ray standing wave fields (e.g. see the review [4] and [5-8]). The combination of GIXB with XSW studies gives new insights into the near surface and interface structure. In GIXB configuration the XSW technique is based on the dynamical X-ray wave fields formed very close to the crystal surface when an incident beam at a grazing angle excites a specular and a diffracted beams from lattice planes perpendicular or nearly perpendicular to the surface (see figure 1). The

GIXB is considered to be dependent on the value of the phase shift between the space periods, as well as of the Bragg angle.

POLARIZABILITY MODEL

Let the reciprocal vector of diffracting crystal net planes is parallel to the direction of ***Ox***-axis. In this case the x-ray diffraction pattern contains the information only about the direction of the ***Ox***-axis. At the same time such pattern is averaged along the directions of the ***Oy*** and ***Oz***-axes. Further we consider the case, when the polarizability $\chi_L(\mathbf{r})$ of perfect crystalline layer with the thickness $T = z_1 - z_2$ is given by the following expression:

$$\chi_L(\mathbf{r}) \equiv \chi_L(x) = \chi_0 + \chi_g \exp(i2\pi x/d) + \chi_{\bar{g}} \exp(-i2\pi x/d), \tag{1}$$

where the parameter d is the period of the polarizability $\chi_L(x)$ i.e. the spacing period of the crystal diffracting net planes. The polarizability of each set of net planes of the natural crystals, as well as of the artificial nanocrystals may be presented by the equation (1). The considered model of the polarizability is valid for description of epitaxial layers, multilayers, low-dimensional structures, liquid crystals, molecular and organic-inorganic hybrid nanostructures, of many types of biological objects etc (see e.g. [1-3]). Formally the deviation from the ideal-elastic scattering (i.e. presence of the absorption in crystalline layer) is described by the complex-valued coefficients

:

$$\chi_0 = -|\chi_{0r}| - i|\chi_{0i}|, \tag{2}$$

$$\chi_g = |\chi_{gr}| \exp(i\eta_g) + i|\chi_{gi}| \exp(i\omega_g), \tag{3}$$

$$\chi_{\bar{g}} = |\chi_{gr}| \exp(-i\eta_g) + i|\chi_{gi}| \exp(-i\omega_g), \tag{4}$$

where

$$-\pi \le \eta_g \le \pi, \tag{5}$$

$$-\pi \le \omega_g \le \pi, \tag{6}$$

Taking into account the relations (2)–(6) the equation (1) may be rewritten in the form below:

$$\chi_L(x) = \chi_r(x) + i\chi_i(x), \tag{7}$$

where

$$\chi_r(x) = -|\chi_{0r}| - 2|\chi_{gr}| \cos\left[2\pi(x + x_\eta)/d\right], \tag{8}$$

$$\chi_i(x) = -|\chi_{0i}| - 2|\chi_{gi}| \cos\left[2\pi(x + x_\omega)/d\right], \tag{9}$$

$$x_\eta = (2\pi)^{-1}(\eta_g - \pi)d, \tag{10}$$

$$x_\omega = (2\pi)^{-1}(\omega_g - \pi)d, \tag{11}$$

Also let assume that the condition $1 >> \left|\sin(\eta_g - \omega_g)\right|$ is fulfilled. Then the equation (9) may be rewritten in the following form:

$$\chi_i(x) \cong -|\chi_{0i}| - 2|\chi_{gi}| \cos(\eta_g - \omega_g) \cos\left[2\pi(x + x_\eta)/d\right] \tag{12}$$

Taking into account the relations (8) – (12), finally the equation (1) may be rewritten as:

$$\chi_L(x) \cong -|\chi_{0r}| - i|\chi_{0i}| - 2\left[|\chi_{gr}| + i|\chi_{gi}| \cos(\eta_g - \omega_g)\right] \cos\left[2\pi(x + x_\eta)/d\right]. \tag{13}$$

The bulk crystal polarizability $\chi_S(x)$ has the same value of the spacing period d, but it has a shift x_0 in a space phase (see figure 1):

$$\chi_S(x) = \chi_L(x - x_0), \tag{14}$$

where

$$0 \le x_0 \le d. \tag{15}$$

INCIDENT WAVE FIELD

In this paper we consider a case, when the stationary part of the incident wave field $\boldsymbol{E}^I(\boldsymbol{r})$ is given by the following equation:

$$\boldsymbol{E}^I(\boldsymbol{r}) = \boldsymbol{E}_o^I \exp(i2\pi\, \boldsymbol{K}^i \boldsymbol{r}), \tag{16}$$

where

$$\boldsymbol{K}^i \boldsymbol{r} = xK_x^i + zK_z^i, \tag{17}$$

$$K_x^i = -K\sin(\theta^i), \tag{18}$$

$$K_z^i = -\sqrt{K^2 - (K_x^i)^2} = -K\cos(\theta^i), \tag{19}$$

$$0 \le \theta^i \le \pi/2, \tag{20}$$

$$|\boldsymbol{K}^i| \equiv K = 1/\lambda = \nu/c, \tag{21}$$

$\boldsymbol{E}_0^i$, $\boldsymbol{K}^I$, K, λ and ν are the amplitude, wave-vector, wave number, wavelength and frequency of the incident plane wave (16) correspondingly; c is the velocity of light in vacuum, K_x^i and K_z^i are the wave-vector $\boldsymbol{K}^i$ projections onto the $\boldsymbol{Ox}$ and $\boldsymbol{Oz}$-axes correspondingly; θ^i is the angle of incidence of the plane wave (16), i.e. $(\pi - \theta^i)$ is the angle, which the wave-vector $\boldsymbol{K}^i$ forms with the $\boldsymbol{Oz}$-axes (see figure 1).

MATHEMATICAL DESCRIPTION OF THE PROBLEM

One of the equations frequently occurring in the problems of the Mathematical Physics, and particularly in the Diffraction Theory is the second-order linear ordinary differential equation with periodic coefficient. The particular case of such equation is the Mathieu differential equation [9-12]. Differential equation with periodic coefficient has manifold applications. Different forms of its periodic solutions emerge in the various branches of natural science and technique, e.g. in the problems of solid state physics [13, 14] and surface states physics [15], holography [16] and integrated optics [17], guiding and diffraction of optical radiation [18-20], physics of multilayer semiconductor microstructures [21], investigations of domain-wall dynamics in ferromagnetic with anisotropy [22], as well as in the problems of x-ray diffraction by the micro and nanoscale materials with periodically modulated polarizability (see e.g. [1-3, 23-28]). The stationary wave field $\boldsymbol{E}^L(\boldsymbol{r})$ inside the crystalline layer is described by three scalar differential equations (see [1]):

$$\left\{\sum_{m=1}^{3}\frac{\partial^2}{\partial x_m^2} + (2\pi K)^2[1+\chi_L(\boldsymbol{r})]\right\}[\boldsymbol{E}^L(\boldsymbol{r})]_n = -\frac{\partial}{\partial x_n}\left\{[1+\chi_L(\boldsymbol{r})]^{-1}\sum_{m=1}^{3}\left\{[\boldsymbol{E}^L(\boldsymbol{r})]_m \frac{\partial}{\partial x_m}\chi_L(\boldsymbol{r})\right\}\right\}, \tag{22}$$

where $n = 1, 2, 3\ldots$, $x_1 \equiv x$, $x_2 \equiv y$, $x_3 \equiv z$ are the variables in the Cartesian coordinate system, $[\boldsymbol{E}^L(\boldsymbol{r})]_m$ are the projections of the vector

$\boldsymbol{E}^L(\boldsymbol{r})$ on the corresponding axes. The magnetic permeability is set equal to unit because we consider only a semiconductor or dielectric structure in this paper. The incident wave field doesn't depend upon *y*, and therefore the set of differential equations (22) is possible to transform to:

$$\left\{\frac{\partial^2}{\partial x^2}+\frac{\partial^2}{\partial z^2}+4\pi^2K^2\left[1+\chi_L(x)\right]\right\}E_y^L(x;z)=0. \tag{23}$$

General solution for transparent crystal

If the absorption is not taken into account, then it is necessary to take

$$\left|\chi_{0i}\right|=\left|\chi_{gi}\right|\equiv 0. \tag{24}$$

For the hard and soft x-rays (i.e. for the values of the wavelength λ ~ *0,1nm ÷ 50nm*) and for semiconductor and dielectric materials the following condition is fulfilled:

$$-\chi_r(x)<<1. \tag{25}$$

One can transform the linear differential equation (23) to the following set of equations:

$$\left[\frac{\partial^2}{\partial u^2}+a-2q\cos(2u)\right]U(u)=0, \tag{26}$$

$$\left\{\frac{\partial^2}{\partial z^2}+(2\pi)^2\left[k^2-(2d)^{-2}a\right]\right\}W(z)=0, \tag{27}$$

where

$$\left[\boldsymbol{E}^L(\boldsymbol{r})\right]_y\equiv E_y^L(x;z)=U(u)\,W(z), \tag{28}$$

$$u=\pi\left(x+x_\eta\right)/d, \tag{29}$$

$$q=(2Kd)^2\left|\chi_{gr}\right|, \tag{30}$$

$$k=K\sqrt{1-\left|\chi_{0r}\right|}, \tag{31}$$

a is proportional to variable separation constant. The equation (26) is well known as a Mathieu equation [9-12]. The application of Mathieu equation to x-ray diffraction problems is a unique theoretical approach, based on the method of construction of eigenvalues and eigenfunctions corresponding to the mathematical model, which describes the x-ray standing wave inside, and outside the diffracting structure. The presented method is correct for the various combinations of the wavelength range from hard x-rays to extreme ultraviolet and the structure space period range from the Angstrom to several hundred nanometers (which we can't say about the generally used diffraction theories). The general solution $E_y^L(x;z)$ of the set of equation (26), (27) in the case of thin layer, i.e. for the region $z_2\le z\le z_1$ may be written in the following form:

$$E_y^L(x;z)=\sum_{m=1}^{2}\int_0^\infty\left[{}^{1;m}D_\mu(q)\,ce_\mu(u;q)+{}^{2;m}D_\mu(q)\,se_\mu(u;q)\right]\times \\ \times\exp\left[i(-1)^m\,2\pi\,z\sqrt{k^2-(2d)^{-2}a_\mu}\right]d\mu, \tag{32}$$

where ${}^{2;\,m}D_0 \equiv 0$. The functions $ce_\mu(u;q)$ and $se_\mu(u;q)$ are the ordinary Mathieu functions of first kind to which the eigenvalues a_μ correspond. The general solution $E_y^S(x;z)$ of the equation system (26), (27) for the bulk crystal, i.e. for the region $z \le z_2$ may be written as:

$$E_y^S(x;z)=\int_0^\infty \left[{}^1G_\mu(q)\,ce_\mu(u+u_0;q)+{}^2G_\mu(q)\,se_\mu(u+u_0;q)\right]\times \times\exp\left[-i2\pi z\sqrt{k^2-(2d)^{-2}a_\mu}\right]d\mu \qquad (33)$$

where ${}^2G_0 \equiv 0$ and

$$0 \le u_0 \equiv (\pi x_0/d) \le \pi . \qquad (34)$$

We search the mathematical expression of electric strength $[\boldsymbol{E}^r(\boldsymbol{r})]_y$ of the reflected x-ray wave field in a Fourier integral form:

$$[\boldsymbol{E}^r(\boldsymbol{r})]_y \equiv E_y^r(x;z)=\int_{-\infty}^{\infty} E_0^r(K_x^r)\exp\left\{-i2\pi\left[xK_x^r - z\sqrt{K^2-(K_x^r)^2}\right]\right\}dK_x^r \qquad (35)$$

Thus we are not doing any supposition concerning the character of the stationary x-ray wave field reflected from the crystal entrance surface $z = z_1$. The only requirement is that the wave fields must satisfy the boundary conditions.

Boundary conditions

If the incident wave field is given by the equations (16)–(21), then the boundary conditions have the following form:

$$E_y^i(x;z_1)+E_y^r(x;z_1)-E_y^L(x;z_1)=0, \qquad (36)$$

$$\left\{\frac{\partial}{\partial z}\left[E_y^i(x;z)+E_y^r(x;z)-E_y^L(x;z)\right]\right\}\bigg|_{z=z_1}=0, \qquad (37)$$

$$E_y^L(x;z_2)-E_y^S(x;z_2)=0, \qquad (38)$$

$$\left\{\frac{\partial}{\partial z}\left[E_y^L(x;z)-E_y^S(x;z)\right]\right\}\bigg|_{z=z_2}=0. \qquad (39)$$

Using the orthogonality conditions of the eigenfunctions involved in (32), (33) and (35) the unknown weight functions ${}^{1;\,m}D_\mu(q)$; ${}^{2;\,m}D_\mu(q)$; ${}^1G_\mu(q)$; ${}^2G_\mu(q)$ and $E_0^r(K_x^r)$, which satisfy the boundary conditions (36) – (39), should be found. One obtains the required expressions of reflected and transmitted wave fields by corresponding substitution of the obtained weight functions into (32), (33) and (35).
fields must satisfy the boundary conditions.

Absorbing crystal

The absorption can be taken into account if the following substitutions are made in the relations presented below:

$$|\chi_{0r}| \to |\chi_{0r}| + i|\chi_{0i}|, \qquad (40)$$

$$\left|\chi_{gr}\right| \rightarrow \left|\chi_{gr}\right| + i\left|\chi_{gi}\right| \cos\left(\eta_g - \omega_g\right), \tag{41}$$

THE RELATIVE INTENSITY OF ENTIRE X-RAY WAVE FIELD OVER THE VACUUM-CRYSTAL SURFACE

The general form of the solutions (32), (33) and (35) is very complicated, therefore we present here and consider only the relations of reflected x-ray wave field $\left[\boldsymbol{E}^r(\boldsymbol{r})\right]_y \equiv E_y^r\left(x; z; x_0; \theta_B; T\right)$ in the particular case, when the angle of incidence $\theta^i = \theta_B$ of the plane wave (16) is satisfying the Bragg condition (see the figure 1):

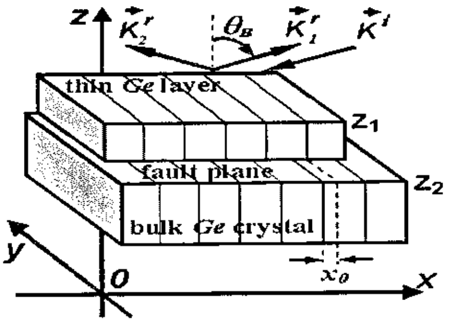

Figure 1. GIXB scheme under the consideration. $z = z_1$ is the crystal entrance surface. Crystal is containing a stacking fault.

Phase shift x_0 exists between space periods of perfect crystalline layer and perfect bulk crystal, which are separated by the fault plane $z = z_2$. $\boldsymbol{K}^i$, $\boldsymbol{K}_1^r$ and $\boldsymbol{K}_2^r$ are the wave-vectors of incident plane wave, specular backdiffracted wave and specular reflected wave respectively. The angle of incidence θ^i of the incident plane wave is satisfying the Bragg condition, i.e. $\theta^i = \theta_B$, where θ_B is the Bragg angle. $\boldsymbol{K}_1^r = -\boldsymbol{K}^i$, wave-vector $\boldsymbol{K}_2^r$ makes an angle $2\theta_B$ with the wave-vector $\boldsymbol{K}_1^r$, $\left|\boldsymbol{K}^i\right| = \left|\boldsymbol{K}_1^r\right| = \left|\boldsymbol{K}_2^r\right| = 1/\lambda$, where λ is the wavelength of the incident plane wave.

$$E_y^r\left(x; z; x_0; \theta_B; T\right) = \sum_{n=1}^{2} E_{yn}^r\left(x; z; x_0; \theta_B; T\right) = C \sum_{n=1}^{2} A_n \exp\left(i2\pi \boldsymbol{K}_n^r \boldsymbol{r}\right), \tag{42}$$

where

$$C \equiv \left|\boldsymbol{E}_0^i\right| \exp\left[i2\pi K\left(x_\eta \sin\theta_B - 2z_1 \cos\theta_B\right)\right], \tag{43}$$

$$\boldsymbol{K}_n^r \boldsymbol{r} \equiv K\left[(-1)^{n+1} x \sin\theta_B + z\cos\theta_B\right], \tag{44}$$

$$A_n \equiv \left[L_1 + (-1)^n L_2\right] \exp\left[i2\pi K(-1)^{n+1} x_\eta \sin\theta_B\right], \tag{45}$$

$$L_1\left(u_0\right) \equiv -\frac{1}{2} + \frac{\cos\theta_B\left[1 + F_1\left(u_0\right) - V_2\left(u_0\right) + i2M_1 p_2\left(u_0\right) W\left(u_0\right)\right]}{\cos\theta_B + M_1 + \left[F_1\left(u_0\right) - V_2\left(u_0\right)\right]\left(\cos\theta_B - M_1\right)}, \tag{46}$$

$$L_2\left(u_0\right) \equiv -\frac{1}{2} + \frac{\cos\theta_B\left[1 + F_2\left(u_0\right) - V_1\left(u_0\right) - i2M_2\, p_1\left(u_0\right) W\left(u_0\right)\right]}{\cos\theta_B + M_2 + \left[F_2\left(u_0\right) - V_1\left(u_0\right)\right]\left(\cos\theta_B - M_2\right)}, \tag{47}$$

$$M_n \equiv \left[(\cos\theta_B)^2 - |\chi_{0r}| + (-1)^n |\chi_{gr}|\right]^{1/2}, \quad (48)$$

$$V_n(u_0) \equiv (\cos\theta_B - M_n)\, W^2(u_0)\, p_n(u_0)\, t_{n+1}(u_0), \quad (49)$$

$$p_n(u_0) \equiv t_n(u_0) / s_n(u_0), \quad (50)$$

$$s_n(u_0) \equiv \cos\theta_B + M_n + F_n(u_0)(\cos\theta_B - M_n), \quad (51)$$

$$t_n(u_0) \equiv M_n \sin(2u_0) \exp[i2\pi KT(M_1 + M_2)], \quad (52)$$

$$F_n(u_0) \equiv (-1)^n W(u_0)[\sin(u_0)]^2 (M_2 + M_1) \exp[i4\pi KTM_n], \quad (53)$$

$$W(u_0) \equiv \frac{M_2 - M_1}{4M_1M_2 + [(M_2 - M_1)\sin(u_0)]^2}, \quad (54)$$

$\boldsymbol{K}_1^r$ is the wave-vector of the specular backdiffracted wave field $E_{y1}^r(x; z; x_0; \theta_B; T)$ reflected from crystal in the direction opposite to that of the incident wave field with wave-vector $\boldsymbol{K}^i$ (see the figure 1); $\boldsymbol{K}_2^r$ is the wave-vector of the specular reflected wave field $E_{y2}^r(x; z; x_0; \theta_B; T)$ and makes an angle $2\theta_B$ with the wave-vector $\boldsymbol{K}_1^r$ (see the figure 1).

The relative intensity $I(x; z; x_0; \theta_B; T)$ of entire x-ray wave field in the vacuum $z > z_1$ is given by the following equation:

$$I(x; z; x_0; \theta_B; T) \equiv \left|E^i(x; z)\right|^{-2} \left|E^i(x; z) + E_y^r(x; z; x_0; \theta_B; T)\right|^2, \quad (55)$$

RESULTS AND DISCUSSION

The images of relative intensity $I(x; z; x_0; \theta_B; T)$ of entire x-ray wave field in the vacuum are calculated depending on the Bragg angle and on parameter x/d in the case $z = 10d$, $T = 200d$, and $x_\eta = z_1 = 0$ (see figures 2 - 4). Relative intensities are computed in the case of incident plane wave of wavelength λ within the region $0{,}178909\text{nm} \geq \lambda \geq 0{,}178899\text{nm}$ i.e. within the $CoK_{\alpha 1}$ line, which is backdiffracted by the (620) planes of absorbing germanium crystal. Thus the wavelength dependence of the polarizability is neglected because the calculations are carried out for a very small range of Bragg angles. One can change the Bragg angle θ_B either by varying the incident radiation wavelength λ or the spacing period d of the polarizability, i.e. by the variations of the sample temperature. The polarizability coefficients are calculated based on data presented in [29].

Image of the relative intensity $I(x; z; \theta_B)$ of entire x-ray wave field over the surface of perfect absorbing germanium crystal extended over volume $0 \geq z$ is presented in the Figure 2.

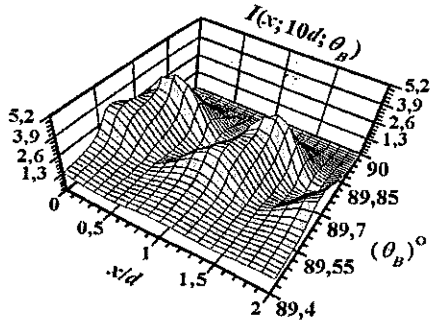

Figure 2. Graphic of the relative intensity $I(x;z;\theta_B)$ of entire x-ray wave field over the surface of perfect single crystal extended over the volume $z_l \geq z$ depending on the parameters x/d and θ_B, where θ_B and λ are the Bragg angle and the wavelength of the incident plane wave respectively. Computations are performed in the case of absorbing germanium crystal and fulfillment of the conditions: $x_\eta = z_l = 0$, $z - z_l = 10d$. Variations of the incident radiation wavelength λ within the region $0{,}178909\text{nm} \geq \lambda \geq 0{,}178899\text{nm}$ changes the Bragg angle θ_B in this figure.

Image of the relative intensity $I(x;z;x_0;\theta_B;T)$ of entire x-ray wave field over the vacuum-crystal surface $z_l = 0$ is presented in the figure 3. Computations are performed in the case of absorbing germanium crystal containing a stacking fault with phase shift $x_0 = d/6$.

Another image of the relative intensity $I(x;z;x_0;\theta_B;T)$ of entire x-ray wave field over the vacuum-crystal surface $z_l = 0$ is presented in the figure 4. Computations are performed in the case of absorbing germanium crystal containing a stacking fault with phase shift $x_0 = d/3$.

Analysis of the equations (42)–(55), as well as of the images presented in figures 2 - 4 shows that relative intensity $I(x;z;x_0;\theta_B;T)$ of entire x-ray wave field in the vacuum $z > z_l$ is modulated periodically along the vacuum-crystal surface $z = z_l$ with the same period d as the crystal diffracting net planes (a short-period modulation). Also the relative intensity $I(x;z;x_0;\theta_B;T)$ of entire x-ray wave field in the vacuum is modulated in the direction normal to vacuum-crystal surface i.e. in the ***Oz***-axes direction. However, in ***Oz***-axes direction the relative intensity modulation period is much longer than the lattice space period d (a long-period modulation). The short-period x-ray intensity modulation along the vacuum-crystal surface gives a possibility to determine the lateral positions of overlaid adsorbed atoms with respect to crystal lattice atoms by combination of GIXB with XSW technique even in the case when the diffracting crystal contains a stacking fault with fault plane parallel to the crystal entrance surface. Also note that if a phase shift x_0 between the space periods of perfect crystalline layer and perfect bulk crystal equals to 0 or d (see figure 2) then the GIXB equations (42) and (55) coincides with the results presented in [1] and [23].

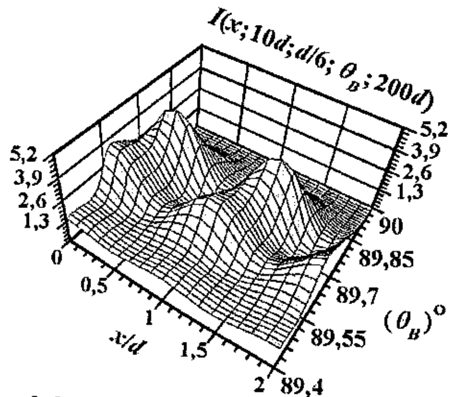

Figure 3. Graphic of the relative intensity $I(x;z;x_0;\theta_B;T)$ of entire x-ray wave field over the vacuum-crystal surface $z = z_l$ depending on the parameters x/d and θ_B, where x_0, θ_B, T and λ are the shift in the space phase, the Bragg angle, the thickness of perfect crystalline layer and the wavelength of the incident plane wave respectively. Computations are performed in the case of absorbing germanium crystal and fulfillment of the conditions: $x_\eta = z_l = 0$, $z - z_l = 10d$, $x_0 = d/6$, $T = z_l - z_2 = 200d$. Variations of the incident radiation wavelength λ within the region $0{,}178909\text{nm} \geq \lambda \geq 0{,}178899\text{nm}$ changes the Bragg angle θ_B in this figure.

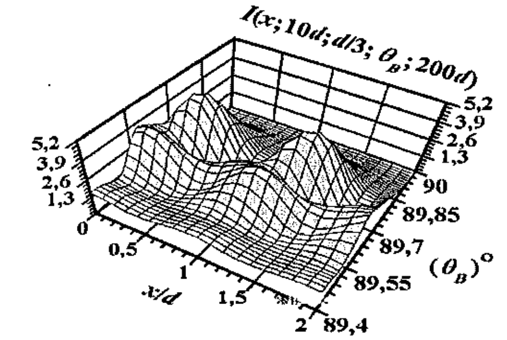

Figure 4. Graphic of the relative intensity $I(x;z;x_0;\theta_B;T)$ of entire x-ray wave field over the vacuum-crystal surface $z = z_l$ depending on the parameters x/d and θ_B, where x_0, θ_B, T and λ are the shift in the space phase, the Bragg angle, the thickness of perfect crystalline layer and the wavelength of the incident plane wave respectively. Computations are performed in the case of absorbing germanium crystal and fulfillment of the conditions: $x_\eta = z_l = 0$, $z - z_l = 10d$, $x_0 = d/3$, $T = z_l - z_2 = 200d$. Variations of the incident radiation wavelength λ within the region 0,178909nm $\geq \lambda \geq$ 0,178899nm changes the Bragg angle θ_B in this figure.

CONCLUSION

Relative intensity (55) of entire x-ray wave field in vacuum is modulated along the crystal entrance surface with the same period d as diffracting net planes of the crystal (a short-period modulation). This gives an opportunity of determination of adsorbed atoms position along ***Ox***-axis with respect to crystal lattice atoms. Thus the combination of GIXB method with XSW technique is also applicable for the surface structure analysis in the case when the diffracting crystal contains a stacking fault with fault plane parallel to crystal entrance surface.

REFERENCES

1. A.P. Bezirganyan, and P.A. Bezirganyan, *Phys. Stat. Sol. (a)* **105**, 345 (1988).
2. A.P. Bezirganyan, Phys. *Stat. Sol. (a)* **109**, 101 (1988).
3. P. A. Bezirganyan, A. P. Bezirganyan and S. E. Bezirganyan, *Phys. Stat. Sol. (a)* **116**, 469 (1989).
4. J. Zegenhagen, *Surf. Sci. Rep.* **18**, 199 (1993).
5. T. Jach, and M.J. Bedzyk, *Phys. Rev. B* **42**, 5399 (1990).
6. T. Jach, and M.J. Bedzyk, *Acta Cryst. A* **42**, 346 (1993).
7. O. Sakata, H. Hashizume, and H. Kurashina, *Phys. Rev. B* **48**, 11408 (1993).
8. O. Sakata and H. Hashizume, *Acta Cryst. A* **51**, 375 (1995).
9. E. Mathieu, J. Math. *Pures Appl. (J. de Liouville)* **13**, 137 (1868).
10. N.W. McLachlan, *Theory and Application of Mathieu Functions* (Dover Publications, New York, 1964).
11. A. Erdelyi, and H. Bateman, *Higher Transcendental Functions*, **Vol.3** (McGraw-Hill Publ. Co., New York, 1953).
12. J. Meixner, F. W. Schaefke, and G. Wolf, *Mathieu Functions and Spheroidal Functions and their Mathematical Foundations* (Springer-Verlag, Berlin, 1980).
13. R.Kronig, and W. Penney, *Quantum Mechanics in Crystal Lattices* (Proc. Roy. Soc. **A130**, London Section, England, 1931), p. 499.
14. L. Brillouin, and M. Parodi, *Wave Propagation in Periodic Structures* (Masson et C[ie], Dunod, Paris, 1956).
15. S.G. Davison, and J.D. Levine, *Surface States in Solid States Physics* - Advances in Research and Applications, **Vol. 25**, edited by H. Ehrenreich, F. Seitz, and D. Turnbull (Academic Press, New York, 1970).
16. H. Kogelnik, *Bell. Syst. Tech.* **48**, 2909 (1969).
17. T. Tamir, *Integrated Optics*, Berlin, New York: Springer-Verlag, 1975.
18. N. S. Kapany and J. J. Burke, *Optical Waveguides*, New York: Academic Press, 1972.
19. M. J. Adams, *An Introduction to Optical Waveguides*, Chichester, New York, Toronto: John Wiley and Sons, 1981.
20. S. Solimeno, B. Crosignani and P. DiPorto, *Guiding, Diffraction, and Confinement of Optical Radiation*, Orlando, New York, London, Tokyo: Academic Press, 1986.
21. M. A. Herman, *Semiconductor Superlattices*, Berlin: Akademie-Verlag, 1986.
22. V. Zarnitsky, I. Mitkov and M. Levi, *Phys. Rev. B* **57**(9), 5033 (1998).

23. A. P. Bezirganyan, Thesis: *The X-Rays and the Extreme Ultraviolet Radiation Dynamical Extreme Diffraction by the Synthesized Multilayer Microstructures*, Yerevan State University, 1990.
24. A. P. Bezirganyan, S. E. Bezirganyan and P. A. Bezirganyan, *The Extinction Length of the X-Rays Diffracted by the One-Dimensional Modulated Structures*, in Proc. 2nd European Symposium on X-Ray Topography and High Resolution Diffraction, Berlin – Gosen, Germany, 1994, p. 77.
25. S. E. Bezirganyan and A. P. Bezirganyan, *X-Ray Specular Standing Wave*, in Proc. 2nd European Symposium on X-Ray Topography and High Resolution Diffraction, Berlin – Gosen, Germany, 1994, p. 78.
26. P. A. Bezirganyan (Jr.), A. P. Bezirganyan, S. E. Bezirganyan and H. A. Bezirganyan (Jr.), *The Standing Wave Formed by Grazing-Incidence X-rays in a Multilayer with Planes Normal to Surface*, in Abstracts XVIII IUCr Congress and General Assembly, Glasgow, Scotland, UK, 1999, P12.OE.001, p. 177; Acta Cryst., A55 Supplement, 1999, P12.OE.001.
27. P.A. Bezirganyan (Jr.), A.P. Bezirganyan, S.E. Bezirganyan and H.A. Bezirganyan (Jr.), *X-Ray Specular Backdiffraction from Thin Crystalline Layer Deposited on the Crystalline Substrate* (Abstracts of Materials Research Society 2001 Spring Meeting R5.4, San Francisco, CA, 2001), p. 322.
28. A.P. Bezirganyan, S.E. Bezirganyan, H.A. Bezirganyan (Jr.) and P.A. Bezirganyan (Jr.), *Investigation $Si_{1-\alpha-\beta}Ge_{\alpha}C_{\beta}/Si$ Strain-Compensated Heterojunction by the X-rays Backdiffraction Method* (Book of Abstracts of EDXRS 2002 Conference, Berlin, Germany, 2002), p. 16.
29. *International Tables for X-ray Crystallography*, Kluwer Acad. Publ., Dordrecht, Boston, London, **Vol. C**, 1992.